From Liposomes to Supported, Planar Bilayer Structures on Hydrophilic and Hydrophobic Surfaces: An Atomic Force Microscopy Study

Jana Jass, Torbjörn Tjärnhage, and Gertrud Puu#
Department of Biomedicine, Defense Research Establishment, SE-901 82 Umeå, Sweden

ABSTRACT The sequence of events involved in the transition from attached liposomes to bilayer patches on hydrophilic and hydrophobic solid supports were visualized in situ by Tapping Mode atomic force microscopy in liquid. In a smooth manner, the attached liposomes spread and flattened from the outer edges toward the center until the two membrane bilayers were stacked on top of each other. The top bilayer then either rolls or slides over the bottom bilayer, and the adjacent edges join to form a larger membrane patch. This is clearly visible from the apparent height of 6.0–7.5 nm of the single bilayer, measured in situ. The addition of calcium appeared to increase the rate of the processes preventing the visualization of the intermediate stages. The same intermediate steps appeared to be present on hydrophobic surfaces, although the attached liposomes seemed to be distorted and the resultant membrane edges were uneven. This work has provided visual and detailed information on liposome coalescence (fusion) onto solid supports and demonstrated how the atomic force microscope can be used to study the process.

INTRODUCTION

Liposomes and black lipid membranes have been the predominant model systems for studies on biological membranes for the past few decades. Although such preparations have many attractive properties and are useful tools for increasing the understanding of processes at and across membrane surfaces, they also have limitations. For example, they are not applicable for performing different spectroscopic analyses. The obvious alternative is to prepare lipid or protein-lipid bilayers on solid supports, a task that many experimentalists have found to be rather complicated. Early attempts to create lipid bilayer structures of natural phospholipids using the Langmuir-Blodgett method were not always successful (Roberts, 1990; Sellström et al., 1992). A typical experience is that the first monolayer is easily deposited; however, during the dipping procedure to produce the second layer, the first layer was stripped off. This behavior is pronounced when doing experiments with the most abundant phospholipid in nature, phosphatidylcholine. A way to circumvent this problem is to deposit the second layer by letting the monolayer-covered support touch the lipid monolayer in the Langmuir trough horizontally.

An alternative, and today more frequently used, method to prepare membrane-like structures on solid supports is to start with liposomes. The method, then called fusion, was described in the 1980s by McConnell et al. (1986). Material can be transferred from the liposomes to both hydrophilic and hydrophobic surfaces. When liposomes hit a suitable solid surface, they may adsorb, break up, and spread to form a bilayer on a hydrophilic surface or a monolayer on a hydrophobic one (Kalb et al., 1992; Nollert et al., 1995; Puu and Gustafson, 1997; Keller and Kasemo, 1998). The interest in how these processes take place, and what driving forces are involved, has increased during the last few years, with emphasis on hydrophilic surfaces (Csúcs and Ramsden, 1998; Pignataro et al., 2000; Reviakine and Brisson, 2000; Zhdanov et al., 2000). Dependent on several factors, such as the surface, the size, and the lipid composition of the liposomes and other experimental conditions, for example the presence or absence of calcium ions, the sequence of the events (adsorption, rupture, and spreading) can be interrupted at any stage. Generally speaking, the density of adsorbed particles must be high for the two last-mentioned steps to take place. Another general conclusion is that it is difficult to get larger areas of a confluent, defect-free lipid bilayer by the liposome method. A deeper understanding of the processes might thus give clues how to prepare a perfect membrane, suitable for such measurements as ion channel activity.

Understanding the process has another, practical implication when working with protein-containing membranes (Contino et al., 1994; Puu et al., 1995; Salafsky et al., 1996). Membrane proteins in liposomes usually have a preferential orientation, for example, an enzyme with the active site directed outwards. It is of course essential that the orientation is maintained in the planar, supported membrane after the reconstitution, for example, in applications such as biosensors (Nikolelis et al., 1999).

The development of the atomic force microscope (AFM) has allowed direct in situ visualization of many biological materials including phospholipid membranes (Shao and Yang, 1995). Imaging has been performed both on Langmuir-Blodgett membranes and membranes deposited from small vesicles (Singh and Keller, 1991; Hui et al., 1995; Shao and Yang, 1995). Most studies in literature have been

Received for publication 10 April 2000 and in final form 15 September 2000.

J. Jass's present address: Department of Microbiology, Umeå University, SE 90187 Umeå, Sweden.

Address reprint requests to Dr. Gertrud Puu, Defense Research Establishment, Department of Biomedicine, SE-90 182 Umeå, Sweden. Tel.: 46-90-1067 37; Fax: 46-90-1068 03; E-mail: puu@ume.foa.se.

0006-3495/00/12/3153/11 $2.00

conducted on lipid films formed and manipulated before introducing the preparation into the microscope. However, one feature of the AFM is that events may be observed by sequential imaging in situ under certain conditions. Some recent works have taken advantage of this. Structural changes were observed when lipid bilayers prepared by Langmuir-Blodgett technique (Hui et al., 1995) or from vesicles (Beckmann et al., 1998) were repeatedly examined. The enzymatic degradation of a phospholipid membrane has been followed in situ (Grandbois et al., 1998). More spectacular changes have been found on preparations with high-density lipoproteins (Carlson et al., 1997) and with lipids (Santos et al., 1998). In these two cases, the scanning process seemed to induce planar bilayer structures from less well defined structures.

Here we report on the use of sequential AFM imaging as a tool to study and visualize the transfer of material from surface-attached liposomes to a surface, eventually building up a bilayer structure. This allows us to capture and recognize the intermediate stages. Although the first observations were made incidentally, a more systematic study was done using hydrophilic and hydrophobic surfaces. A liposome preparation was selected for its rather slow transfer kinetics to be able to grasp different stages. A similar AFM approach was recently reported (Reviakine and Brisson, 2000).

MATERIALS AND METHODS

Chemicals

1,2-Dipalmitoyl-*sn*-glycero-3-phosphocholine (DPPC), 1,2-dipalmitoyl-*sn*-glycero-3-phosphoethanolamine (DPPE), and cholesterol were from Avanti Polar Lipids (Alabaster, AL), whereas 1,2-dipalmitoyl-*sn*-glycero-3-phosphoglycerol (DPPG), 1,2-dipalmitoyl-*sn*-glycero-3-phosphate (DPPA), and galactosylcerebroside (type II) were from Sigma (St. Louis, MO). The nicotinic acetylcholine receptor from *Torpedo nobiliana* was purified and biotinylated as described recently (Puu et al., 2000). Water was taken from a Milli-Q Plus 185 (Millipore, Molsheim, France) ultrapure water system with a resistivity of >18 MΩcm. Polished 100-oriented, boron-doped silicon wafers were from Aurel, Landsberg, Germany.

Tris-HCl (20 mM) with 100 mM NaCl and 0.02% sodium azide, pH 7.4, was used as buffer for preparing liposomes and for the subsequent incubations.

Atomic force microscopy

A Digital Instruments (Santa Barbara, CA) Nanoscope III AFM fitted with a 125-μm scanner (J-scanner) and a Tapping Mode liquid cell was used to image coalescence of liposomes in situ. Standard Si_3N_4 tips with a nominal force constant of 0.35 N/m were used and the forces were minimized during the scans. The scanning line speed was optimized between 1.5 and 3.5 Hz with a pixel number of 256×256, depending on the scan size. Images were recorded in both height and amplitude modes. Height images were flattened and plane adjusted. All measurements were done on the height images; however, the processes were easier to visualize in the amplitude mode.

For imaging samples after an overnight incubation with liposomes or when starting with monolayer-covered substrates, the slides were carefully cut (10×10 mm) and affixed to a magnetic disk by adhesive tabs (Agar Scientific, Cambridge) without allowing the surface to dry. When imaging liposome attachment and coalescence to a clean surface, the slides were affixed to a magnetic disk and placed directly into the microscope. A glass Tapping Mode liquid cell was assembled over the samples without the O-ring, and the solution (liposomes or calcium) was added by Hamilton syringe in the gap where the O-ring sits, between the cell and the sample.

The area measurement of the bilayer patches were performed on a PC using the UTHSCSA ImageTool program (developed at the University of Texas Health Science Center at San Antonio, San Antonio, TX, and available from the Internet by anonymous FTP from maxrad6.uthscsa.edu).

Liposome preparations

Liposomes were prepared by detergent depletion techniques, with *n*-octylglucoside as the detergent (Puu and Gustafson, 1997). In short, lipids were dissolved in chloroform or chloroform/methanol, deposited on the wall of a round bottom flask by evaporation of the solvents, and dissolved again in buffer containing 110 mM *n*-octylglycoside at 40°C.

The galactosylcerebroside-containing liposomes consisted of DPPC, DPPE, DPPG, and cholesterol at 40, 25, 20, and 5 mol %, respectively, and 10% of the glycolipid. The total amount of lipids was 16 μmol and the final concentration of lipids in the liposome preparation 2 mM. Detergent was removed by extensive dialysis, using a Spectropor dialysis membrane with a cutoff of 3500.

Preparations with the receptor had a slightly different lipid composition, with 35, 25, 20, and 20 mol % of DPPC, DPPE, DPPG, and cholesterol, respectively. Approximately 1 mg of protein was added to 16 μmol of lipid mixture, together with the detergent. Detergent removal was in this case performed by gel chromatography. Liposome-containing fractions were identified by light scattering and pooled.

Liposomes and proteoliposomes prepared with these methods generally result in unilamellar vesicles with a diameter of 200–400 nm (Mimms et al., 1981). Simple light-scattering experiments indicated the same magnitude.

Substrate preparation

Silicon slides were cut and cleaned following procedures reported (Puu and Gustafson, 1997). For the study on proteoliposomes, the slides were preincubated with vesicles before being transferred to the AFM cell (Puu et al., 2000). This preincubation took place in standard 4-ml polystyrene photometer cuvettes, containing buffer with 10 mM $CaCl_2$ and proteoliposomes giving a lipid concentration of $\sim$0.1 mM. Incubation took place overnight at room temperature with constant stirring. The slides were withdrawn from the cuvettes and washed repeatedly with calcium-free buffer. Membrane thickness was measured by ellipsometry, and the slides were then prepared for AFM.

Most studies were performed without preincubation outside the microscope. A slide containing a hydrophobic or hydrophilic surface was positioned in the AFM liquid cell, and the background (surface without liposomes) was imaged in calcium-free buffer. Scanning was stopped, and 10 μl of a liposome suspension (lipid concentration 0.4 mM for the hydrophilic surface) was carefully injected with a Hamilton syringe into the liquid cell. The tip was vibrated for 5 min for sample mixing and the incubation was allowed to proceed for approximately 1 h before imaging was initiated.

Hydrophobic slides were prepared with a monolayer of DPPA using the Langmuir-Blodgett technique at a pressure of 45 mN/m. Thickness was estimated by elliposometry and the hydrophobicity from visual inspection of the shape of a droplet of buffer on the surface. The surface was also inspected by scanning in the AFM to check for spontaneous bilayer formation, which could take place upon storage for several hours. Only bilayer-free surfaces were used for subsequent experiments with liposomes. A 7-μl volume of a more concentrated liposome suspension, 2 mM, was used.

Calcium was added to some experiments. A 3.5-μl volume of 200 mM $CaCl_2$ solution was injected by Hamilton syringe into the cell. Imaging was resumed.

RESULTS

Proteoliposomes on a hydrophilic surface

Sequential imaging in the AFM of bilayer formation from liposomes was initiated by an observation made during a study on membrane protein stability and distribution in lipid layers on solid supports (Puu et al., 2000). We had prepared liposomes with biotinylated nicotinic acetylcholine receptor, as well as control proteoliposomes with unmodified receptor. The transfer of material from these proteoliposomes onto the solid surface took place overnight, as described in Materials and Methods. The presence of receptor molecules with correct orientation was shown by radiolabeled streptavidin and by α-bungarotoxin binding (Puu et al., 2000). Some of the slides were incubated with streptavidin-colloidal gold particles (20 nm) and washed before transfer to the liquid cell, whereas others were transferred directly. Both samples resulted in similar AFM sequences of events. A preparation that had been exposed to streptavidin-gold particles, although none was detectable within the displayed areas, was used for the series in Fig. 1, as this sequence turned out to be the most complete, informative, and clear of all recorded.

During AFM imaging of these preparations, we noticed that large areas were covered by a rather smooth lipid film, easily distinguished from the more rough silica surface (Fig. 1 *A*). We also noticed the presence of intact, attached liposomes on the silica surface, despite the preincubation and washing procedure that should have removed loosely bound material. By sequentially capturing nine images in the liquid cell with an interval of 101 s, we observed how some intact liposomes were flattened and formed a film structure (Fig. 1, *B–I*). The figure legend describes the process in detail. Briefly, the initially adsorbed liposomes seemed to collapse from the outer periphery toward the center of the liposome. The partly flattened liposome in Fig. 1 *C* had a height of 12.0 $\pm$ 1.6 nm ($n = 5$) at the edges, indicating that the liposome was likely collapsing onto itself to produce a double-bilayer structure. This process continued until the whole liposome had collapsed to produce two bilayers stacked on top of each other (Fig. 1, *B–G*). At this point the double-bilayer disk suddenly coalesced (fused) with already formed bilayer patches (Fig. 1 *H*) and its thickness changed to that of a single bilayer (II). The height of the lipid membrane imaged under these conditions was 5.9 $\pm$ 0.6 nm ($n = 5$) at the final stage (Fig. 1 *E* cross section). Although it is difficult to see, a transition state is present in Fig. 1 *D* where, halfway up the double-bilayer disc, the height was reduced to a single bilayer. The coalescence of the lower half of the liposome with the membrane at the bottom of the image was not captured in this frame as the scan direction was going up the image, but it is visible in the next figure (Fig. 1 *F*). The mechanism of spreading is not clear in this sequence, but we believe that the subsequent experiments performed help elucidate the intermediate stages of the process.

After the initial liposome flattening and spreading into a bilayer membrane (Fig. 1, *C–F*), the second liposome then follows the same process (Fig. 1 *G*). The process appears to occur when the edge of the resultant membrane of the first liposome spreads up to the edge of the next liposome. Thus the spreading of the three liposomes to form a membrane bilayer occurs in succession, possibly initiated by the contact between the membrane edges of the liposomes.

The unique feature of this sequence of images illustrates how adjacent bilayer patches unite and form a larger, continuous bilayer (Fig. 1, *G–I*). When one liposome collapses and forms a bridge between the two bilayer patches, (Fig. 1, *G* and *H*) a wedge of uncovered silica is formed (middle lower part of Fig. 1 *H*). Between the images in Fig. 1, *H* and *I*, that region is filled. We do not notice any more lipid spreading from liposomes within the image. However, material may be transported to and from other parts of the surface into our field of view, thus causing further spreading of the membrane bilayer.

This sequence contains many of the features that could be seen in subsequent experiments and was the most comprehensive one, despite the fact that the tip had a small artifact. The tip artifact, which may be due to tip contamination or a tip imperfection, is manifest primarily at the edges of the bilayers. It appears as an extra step of approximately the same height of a single bilayer (Fig. 1 *B*, arrow), however, we have verified that it is an artifact by finding similar effects on some small imperfections in the bilayer located within the circles in Fig. 1 *B*. The artifact is enhanced in the deflection mode, although it does not alter the height data.

The size of the proteoliposomes were estimated to be 200–400 nm (see Materials and Methods). When adsorbed to the surface, the dimensions were approximately 89 $\pm$ 18 nm ($n = 10$) in height and 315 $\pm$ 47 nm ($n = 10$) in diameter, giving a height-to-diameter ratio of $\sim$0.3. This suggests that the liposomes tended to spread as they adsorbed to the surface or due to some pressure produced by the tip during scanning. The images were taken in Tapping Mode at the lowest possible forces, although this may be enough to stimulate some spreading of the liposomes.

Glycolipid-containing liposomes on a hydrophilic surface

For a more systematic investigation, we chose to work with a protein-free liposome preparation, with the same phospholipid components as in the proteoliposomes but containing 10 mol % galactosylcerebroside and less of cholesterol. The effects of varying the ratios of the lipid components and of membrane proteins on kinetics for planar bilayer mem-

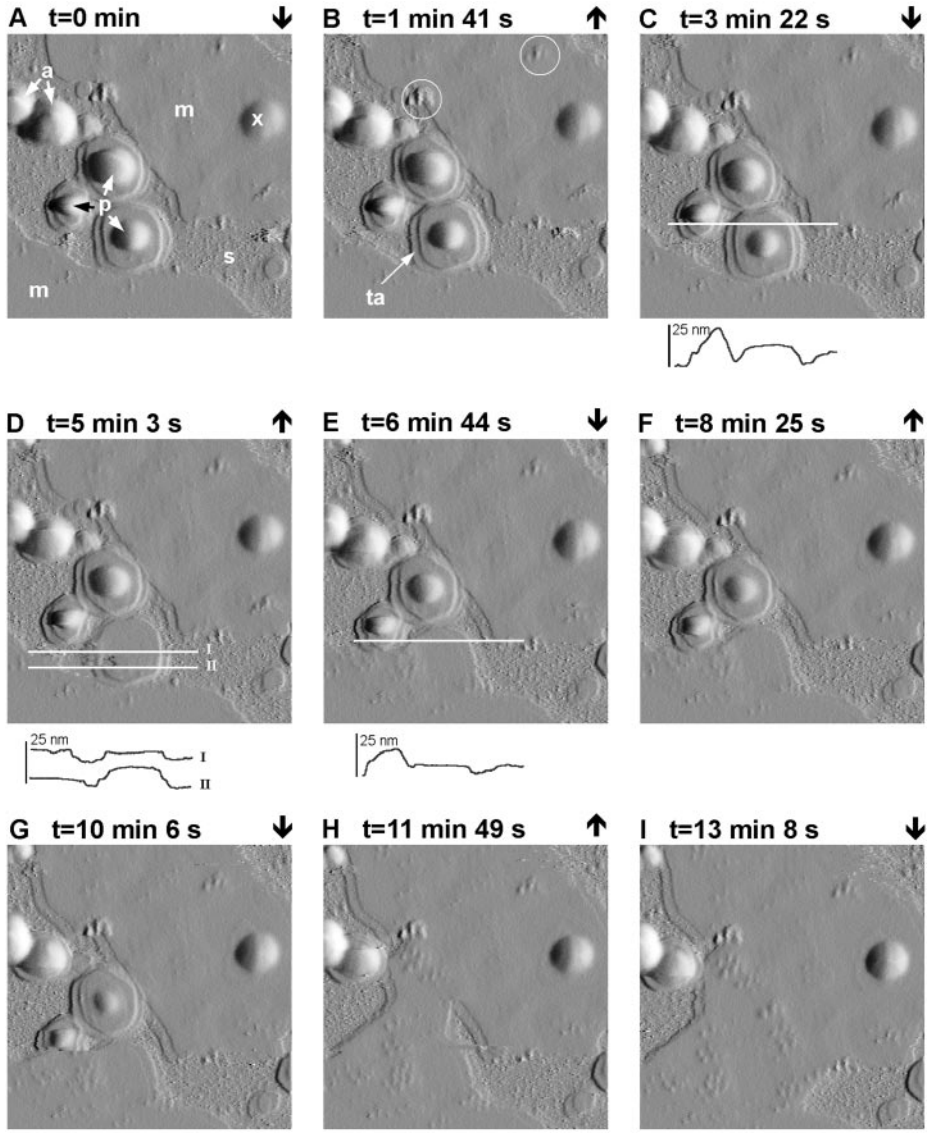

FIGURE 1 A sequential series of AFM images demonstrating proteoliposome flattening, rupture, and spreading on a hydrophilic surface (silica). The images, collected in Tris-HCl/NaCl buffer (pH 7.4), are presented in the amplitude mode. (*A*) The attached liposomes (*a*), partially flattened liposomes (*p*), and lipid bilayers (*m*) are clearly distinguished from the bare silica surface (*s*). The three partially flattened liposomes (*p*) in the center of the image slowly spread through frames *A* to *C*, until the central region is flattened in the lower liposome, as seen in *D*. The cross section of the area identified by the line (measured from height images) shows the height of the flattened region of the liposome in *C* is 11.6 nm, approximately twice that of the resultant membrane height of 5.6 nm measured in *E*. *E* also shows that the height of the newly formed disk is apparently the same as the adjacent membrane originally present. As the scan moves half-way up the liposome in *D*, the height of the flattened liposome is reduced from a double bilayer at the bottom (*II*) to a single bilayer at the top (*I*). (*E*) We find that the lipid material spread down toward the lower membrane and the second liposome, thus preventing us from seeing this in the previous frame. As the membrane material spread toward the remaining two partially processed liposomes, they begin to coalesce in succession and in the same manner through frames *G* to *I*. Eventually the lipid bilayer membrane spreads to cover most of the silica surface in our view. The last two frames, *H* and *I*, also show that edges of the bilayers close to each other rearrange to produce a confluent membrane. When comparing the attached liposomes (*a*) in the first (*A*) and the last (*I*) frames, we observe the slow flattening at the edges as seen with the three processed liposomes. Throughout the sequence, there is a liposome (*x*) in the right upper region of the frame that does not change and appears to be trapped beneath the membrane. (*B*) We have identified the tip artifact manifest as a step-wise edge to the partially flattened liposomes by an arrow. The tip artifact is established by the same type of pattern exhibited by the different circled imperfections in the membrane. All scan sizes are 1.67 $\times$ 1.67 μm and the arrows along the side of the frames indicate the slow scan direction.

brane formation on silica was studied earlier (Puu and Gustafson, 1997). Generally, these mixtures were shown to have a slow kinetics, much slower than, for example, liposomes composed of dioleoyl-phosphatidylcholine only. The rates could be increased and the planar membrane formation brought to completeness by addition of calcium ions. The

lipid composition with the lowest bilayer formation rate on silica, hardly detectable with ellipsometry, was modified to contain a low amount of the glycolipid. With this preparation, both bilayer patches and attached liposomes could be observed at the start of imaging.

The protocol was changed from the proteoliposome experiment, in that no overnight preincubation took place. The liposomes were injected directly into the liquid cell and were present in the buffer throughout the experiment. Not only did this allow us to image the clean silica surface before the start of the experiment, but it also provided the maximum opportunity to capture the events and reduced a large background of already deposited material. Therefore, throughout the experiments we could see adsorption and detachment of liposomes. In a few cases, adsorbed liposomes were moved around the surface by the AFM tip.

Two separate AFM sequences (Figs. 2 and 3), demonstrating the coalescence of liposomes on a hydrophilic silica surface, were chosen so that all of the intermediate stages could be clearly captured and presented. Fig. 2 *A* is a low magnification of an area where the different stages are visible, showing intact adsorbed liposomes, already formed bilayer patches, and intermediate forms. The area outlined (in a box) draws attention as it provides clues as to how an attached flattened liposome might produce a single-bilayer structure. This region was magnified in Fig. 2, *B–E*, by AFM software and studied in more detail. The images demonstrate how a flattened liposome clearly consisting of two bilayers suddenly starts to move and split to the right and left as it simultaneously moves toward the top of the image. Finally, the process continues and a larger area of a single-bilayer thickness is obtained (Fig. 2 *E*). The cross-sectional analysis in Fig. 2 *B* shows step increments that are interpreted as two bilayers with a total height of 15.5 nm, and after spreading in Fig. 2 *E*, there is only one bilayer of 7.4 ± 0.4 nm ($n = 8$).

The arrow at the top of the figure shows the slow scan direction of each image. It appears that the tip may aid in initiating the lipid movement; however, after that, the motion of the top layer seems to occur in a single direction

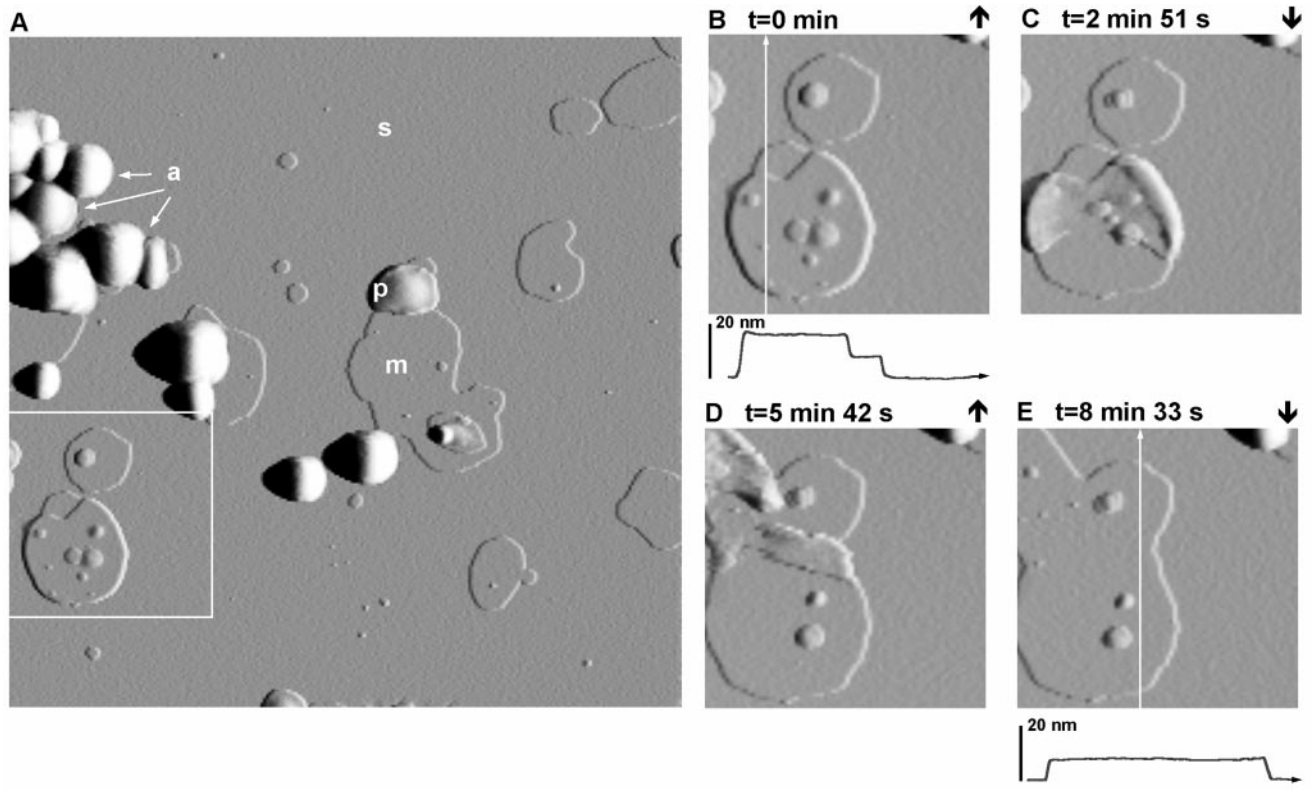

FIGURE 2 AFM sequence capturing the intermediate states during planar bilayer formation from glycolipid-containing liposomes on a hydrophilic surface (silica). The images are collected in Tris-HCl/NaCl buffer and presented in the amplitude mode; however, cross sections and measurements are done in the height mode. This sequence shows the top bilayer of a flattened liposome collapsed and moving over the bottom bilayer before it produces a single confluent lipid membrane. (*A*) A 10-μm scan shows a number of different stages of the process, including attached liposomes (*a*), partially flattened liposomes (*p*), and membrane disks (*m*) on the silica surface (*s*). The sequence in *B* through *E* occurs in the outlined box (3 μm $\times$ 3 μm). The cross section in *B* shows that the disk is composed of two bilayers (7.8 nm each) on top of each other, with a total height of 16 nm. (*C* and *D*) The top layer moves over the bottom layer to the silica surface and coalesces to form the single bilayer structure seen in the cross section of *E*. The slow scan direction is indicated by the large arrows above each image.

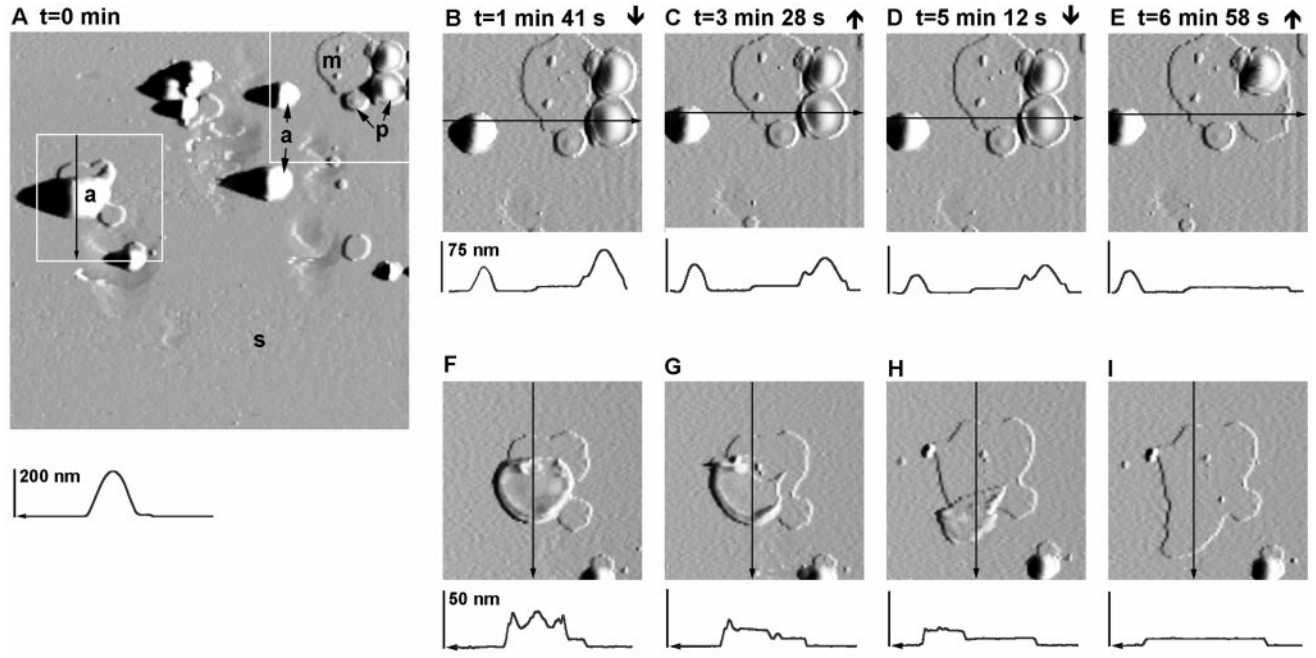

FIGURE 3 AFM images capturing the intermediate stages of glycolipid-containing liposome rupture and spreading on hydrophilic silica surface of two independent events in the same field of view. The images, collected in Tris-HCl/NaCl buffer, are presented in the amplitude mode, and all cross sections and measurements are done in the height mode. (*A*) Overview of a surface containing attached liposomes (*a*), partially flattened liposomes (*p*), and coalesced bilayer disks (*m*) on the silica surface (*s*). Two short sequences of 3.5-μm scans outlined in the boxes show two events occurring simultaneously in a 9-μm scan. (*B–D*) Partially flattened liposome spreading until it coalesces to the silica surface to form a confluent membrane disk in *E*. The cross sections from these images follow the partially flattened liposome in *B* showing that the edge of the liposome has the height of a double bilayer (14 nm) with an adjacent single bilayer membrane (7.0 nm) in *C* and *D*. The liposome transforms by *E* to a single bilayer (6.2–6.5 nm). The second sequence (*F–I*) demonstrates the intermediate stages where an attached but not fully flattened liposome forms a bilayer. In *A*, the cross section shows the height of an attached liposome of ~190 nm. The liposome collapses so that the two bilayers are not fully flattened on top of each other as depicted in the cross section of *F* with heights ranging from 16 nm to 40 nm. The area of the double bilayer and the adjacent disk is 3.4 μm^2. (*G* and *H*) The top bilayer begins to move over the bottom layer. The process is complete by *I* where the remaining membrane disk is a single bilayer with a thickness of 6.5 nm and an area of 3.1 μm^2. The arrows at the top of each frame indicate the slow scan direction.

regardless of the scan direction. The images were collected using Tapping Mode thereby reducing the drag forces of the tip as may be found in the contact mode.

Fig. 3 contains two separate events showing different intermediate stages occurring simultaneously in one field of view. The first image (Fig. 3 *A*) is an overview of the scan area showing the different stages, including attached liposomes, partly flattened liposomes, membrane sheets, and bare silica surface. One sequence (Fig. 3, *A–E*) shows a similar intermediate state to that observed in the proteoliposome preparation (Fig. 1), where a partly flattened liposome slowly collapses from the outer edges and forms a bilayer. The cross sections clearly show the decrease in height of the liposome center from nearly 75 nm to the height of a double bilayer, 15 nm, as observed at the edges. The change from the double bilayer in Fig. 3 *D* to a single bilayer in Fig. 3 *E* is not imaged in this sequence; however, the second series shows more detail of the intermediates. This sequence (Fig. 3, *A* and *F–G*) shows the collapsing of a liposome onto itself and the intermediate stages in the formation of a bilayer membrane. The cross sections show that the intact liposome (Fig. 3 *A*) of ~190 nm decreases in height to form an irregular surface with the lowest region at 16 nm and the highest point of 40 nm (Fig. 3 *F*). The lowest point of the collapsed liposome in Fig. 3 *F* (16 nm) closely corresponds to the height of a double bilayer if a single bilayer were 6.5 nm. The cross sections of the subsequent images (Fig. 3, *G* and *H*) clearly show the step profile of the two stacked bilayers. The top bilayer appears to move over the bottom bilayer without completely collapsing as in the previous figure sequence (Fig. 2). It is clear that a single bilayer results in Fig. 3 *I* with a height of 6.2–6.5 nm.

The dimensions of various structures present in the images were measured by cross section analysis performed in the fast scan direction of the height images. Estimations of the liposome sizes were made from attached liposomes under the imaging conditions outlined in the methods section. The measured values for the diameter may be overestimated due to the properties of the tip. The height measurements may also be influenced by the tip forces, although they were minimized by using Tapping Mode. The average height of the glycolipid liposomes in two separate experi-

ments was 249 ± 75 nm ($n = 11$) and 264 ± 68 nm ($n = 6$), respectively. The height-to-diameter ratio was approximately 0.3 in both experiments, which suggests that the liposomes were not attached as hemispheres but were flattened. The dimensions also suggest that the intact liposome as a sphere should have a diameter of several hundred nanometers. We may have a heterogeneous size distribution of the liposomes or there had been liposome-to-liposome fusion, preferably between surface-bound vesicles (Reviakine and Brisson, 2000), during the preincubation.

Effects of calcium ions

Calcium ions appear to facilitate as well as increase the rate of planar membrane formation from liposomes (Puu and Gustafson, 1997; Reviakine and Brisson, 2000). After collecting the images in Fig. 2, a small volume (3.5 μl) of 200 mM calcium chloride was injected into the liposome suspension to give an approximate concentration of 4.5–7 mM. Images were difficult to obtain under these conditions as the calcium ions introduced a tip-surface interaction, which resulted in high noise. The presence of high background noise was also found when working with a calcium-containing buffer and a clean silica surface, with no lipid material. It was impossible to capture the transition states between intact liposome and bilayer structures. The reconstitution was identified indirectly. Between images, attached liposomes disappeared and new areas of lipid bilayer islands appeared. The presence of calcium resulted in membranes with an apparent height of 4.0 ± 1.0 nm ($n = 13$), which is much lower than in the other experiments (Müller and Engel, 1997). This may be caused by greater tip forces required to track the surface due to tip-surface interactions, although the value is closer to what could be expected for a lipid bilayer structure.

Glycolipid-containing liposomes on a hydrophobic surface

A hydrophobic surface was created by coating a silica slide with a monolayer of DPPA, in the presence of calcium ions, before the introduction of glycolipid-containing liposomes. The kinetics on lipid-covered silica is much faster, by a factor of 5–10, than on silica for liposomes with similar lipid compositions as used here (Puu and Gustafson, 1997). This behavior was verified for the galcer-containing liposomes, using an optical, resonant mirror biosensor equipped with a hydrophilic or a hydrophobic cuvette. On-rates were ~10 times higher on the hydrophobic sensor surface.

When starting imaging in the AFM, after ~1 h of incubation, we found much more material deposited on the monolayer than in experiments with bare silica. Furthermore, we found that surface structures, such as attached liposomes, partially flattened liposomes, and membranes (Fig. 4), appeared significantly different. The attached liposomes were distorted and irregular in shape. The height of the liposomes was 142 ± 64 nm ($n = 10$) and the height-to-diameter ratio was only 0.17 ± 0.07 ($n = 10$), half of the values obtained in the other experiments, and was due to a reduction in the apparent height. Images were collected in both trace and retrace in the fast scan direction (across the image). When superimposing these two images we observed no unusual differences that could be attributed to high forces exerted by the tip. If the liposomes were leaning in opposite directions we would have suspected high forces to be involved in the reduced height of the liposomes. We did not observe this phenomenon; therefore we attribute the flattening of the liposomes to be primarily due to the substrate-liposome interactions.

The membrane structures (Fig. 4, *A* and *F*) were irregular, and often very small patches and long thin strands of lipid membrane were present in addition to membrane sheets. Many small lipid particles were also observed on the surface of the membranes (Fig. 4 *F*). Small lipid debris were also recognized in experiments with silanized, hydrophobic surfaces (data not shown), indicating that such material likely originated from the liposomes than from the pre-deposited monolayer of DPPA.

The sequence of images in Fig. 4 demonstrates the process of three separate liposomes onto a DPPA monolayer. The adsorbed liposome z first flattens (Fig. 4 *A*) and then appears to collapse on top of itself (Fig. 4 *B*) before spreading to form a lipid membrane (Fig. 4 *C*). Sudden changes in the height, as shown by cross sections, suggest that the transition events occur rather rapidly even though the overall transfer occurs at about the same rate as on the hydrophilic surface (6−8 min). Liposome y (Fig. 4 *A*) also proceeds in the same manner, by flattening (Fig. 4, *A–D*) and eventually collapsing on top of itself (Fig. 4 *E*). However, the transition structure between the collapsed liposome and the final single-bilayer membrane is not captured at any instance under these conditions (Fig. 4 *F*).

To determine whether the liposomes spread onto the DPPA surface as a monolayer or bilayer, a defect was scratched into the lipid surface. The resulting height from the silica surface to the top of the lipid layer was 9.1 ± 1.5 nm. In previous scans, the first bilayer on the surface was 6.8 ± 0.3 nm and the second bilayer was 7.9 nm, with a final height of 14.6 nm. These measurements suggest that the thickness from the silica surface is equivalent to one and a half bilayers (or a monolayer and bilayer).

DISCUSSION

The results presented here fill a gap in understanding the events involved in formation of a planar, supported lipid bilayer from liposomes. The process is usually divided into a number of steps: adhesion, liposome flattening, rupture, and formation of a planar single-bilayer structure. We were

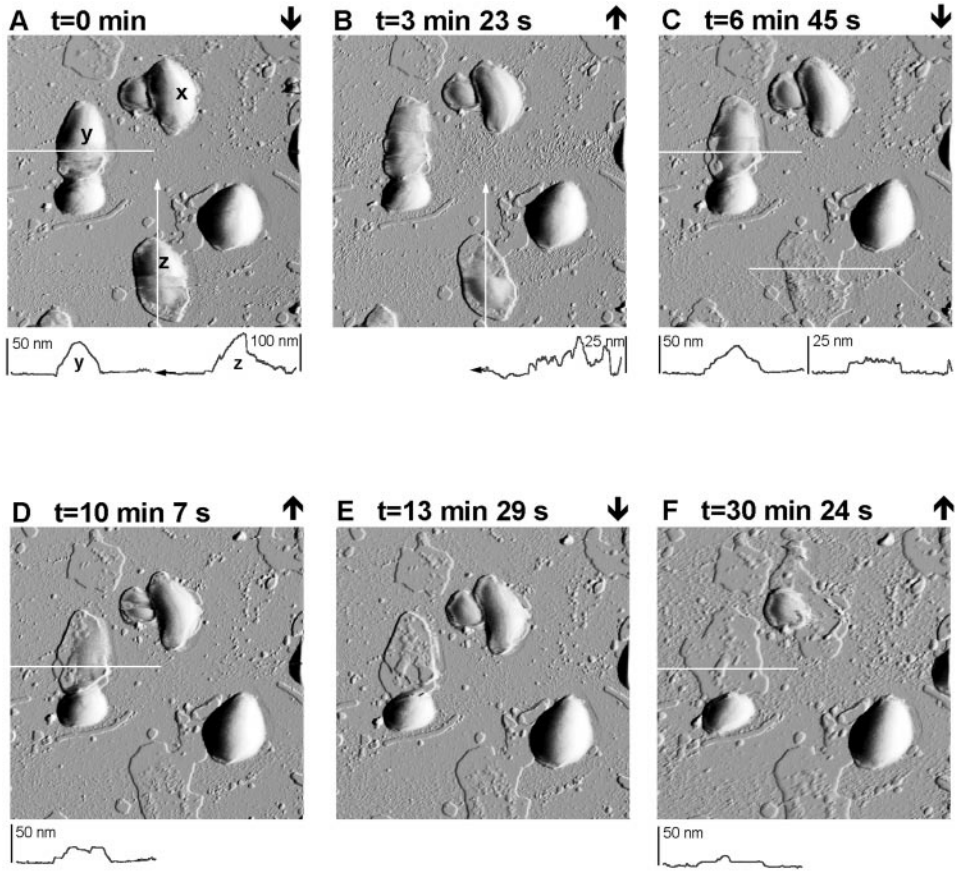

FIGURE 4 An AFM sequence of the coalescence of glycolipid-containing liposomes on a DPPA lipid monolayer creating a hydrophobic surface. The images were collected in Tris-HCl/NaCl buffer and presented in the amplitude mode; however, all measurements are determined in the height mode. (*B*) Liposomes attached to this hydrophobic surface appeared irregular and deformed. (*A*) Liposome x in *A* slowly flattens through *B–E*, until a bilayer disk is formed in *F*. It is adjacent to a smaller liposome that does not change, and the bilayer is formed around the smaller liposome, visible in *F*. The cross section of liposome z in *A* decreases in *B* until a bilayer of 6.5 nm is present in *C*. The cross section of liposome y in *A* also demonstrates the slow flattening until distinct 7-nm steps, suggesting that three bilayers are stacked on top of each other in *D*. These bilayers then spread to form a single bilayer by frame *F*. The images were collected at regular 3-min and 23-s intervals, but four images between *E* and *F* are not shown as they contained no new events. The resultant membranes appeared to have irregular edges and contain small particles of approximately bilayer height that may have been trapped beneath the final membrane. The slow scan direction is indicated by the arrow at the top of each frame.

able to catch not only gross structural changes but also several intermediate states. The results suggest that once the process is initiated, it is a smooth and continuous chain of events. We chose to work with liposomes with slow kinetics to increase the probability of visualizing changes continuously within the time frame given by the relatively slow scanning speeds of the AFM. The slow adsorption kinetics was evident from the fact that too few liposomes were attached instantaneously (Zhdanov et al., 2000); therefore, scanning was started after ~1 h when there was a substantial population of liposomes on the surface. The liposomes were prepared by detergent depletion techniques, which generally result in rather large unilamellar vesicles, with a diameter of at least 200 nm. Even bigger liposomes were found in the AFM study, which indicates that there had been a liposome-to-liposome fusion and/or that the size distribution in the liposome preparation was broad. Another feature of the liposomes, which might be of some relevance for the results, is the presence of hydrophilic parts extending from the liposomal membrane to the aqueous surroundings. In the glycolipid-containing liposomes the galactosylcerebroside occupies ~10% of the liposome surface area, whereas the receptor occupies ~5% in the proteoliposomes.

According to prevalent theories (Reviakine and Brisson, 2000; Pignataro et al., 2000), one would expect these rather big liposomes to adsorb and flatten to a pancake-like structure, followed by rupture to end up as single-bilayer disks by spreading. A schematic, unifying representation of our observations is given in Fig. 5. For simplicity, the scheme is drawn as the events for a single, isolated liposome, although the results indicate the importance of contact points between adjacent membranes (see below). We notice that the liposome is flattened from the outside toward the center until it completely collapsed onto itself. Also, some spreading takes

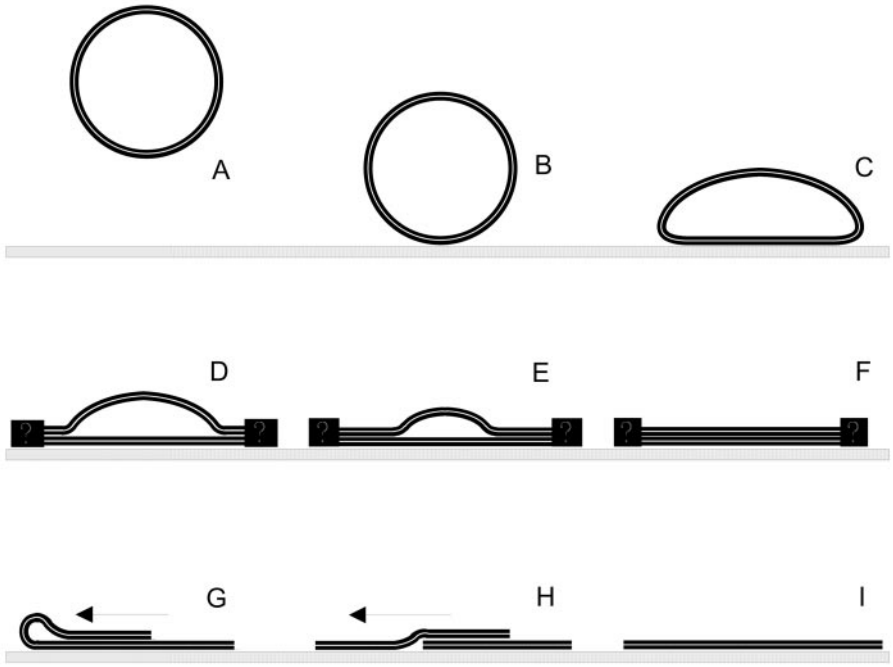

FIGURE 5 A simple and unified interpretation of the transformation from liposome to supported planar bilayer as suggested by the AFM sequences. The liposome approaches (*A*), adsorbs (*B*), and attaches (*C*) to a surface. As attached, it begins to flatten from the edges (*D*). The outer, flattened areas expand and spread (*E*), resulting into a partially flattened liposome (*D* and *E*). The liposome collapses to form two bilayers (*F*) stacked on top of each other. The uppermost bilayer moves from the lower one to unoccupied areas on the surface. This movement can occur by two mechanisms, rolling as in *G* and sliding as in *H*, in both cases resulting in a single bilayer structure (*I*). The edges are marked as boxes, as the AFM images are not clear enough to give information about the structure and organization at the boundaries. The edge-to-edge effects between adjacent membrane structures, which might be a requisite for the process or at least speeds it up considerably, are not included in this simplified scheme.

place during this flattening process. The areas of one- or two-bilayer-thick membranes are slightly increasing simultaneously with shrinkage of the liposome. This process results in two bilayer structures, one on top of the other, formed as disks of about the same size. The resolution in the images does not allow us to follow what is happening at the edges (marked as boxes) and we cannot tell whether the layers are connected or free. The transit to a single bilayer takes place in a way that in some images can be interpreted as sliding (Fig. 5 *H*). In other cases we would rather interpret the movement as rolling (Fig. 5 *G*), showing great similarity to the tank-tread-like motion observed by Rädler et al. (1995), which implies some connection between the layers. The sliding/rolling results in temporary accumulation of the lipidic material at the edges of a disk.

In a recently published Monte-Carlo simulation (Zhdanov et al., 2000), the effect of an autocatalytic process (lipid-induced decomposition) on the kinetics and on the coverage of lipidic material from adsorbed vesicles was shown to be important. We noticed that edge-to-edge contacts between flattened liposomes, stacked membranes, and/or single bilayers seem to stimulate the rate for bilayer formation. This could at least partially explain why we observed similarities in the events on hydrophobic and hydrophilic surfaces. In both systems we had bilayer patches near the spreading liposomes, suggesting that this may be a distinct process occurring after the initial lipid deposition to the surface. If that is the case, then the effects of the different surfaces on liposome fusion would be more important in the initial events, which were rapid on the hydrophobic surface. Subsequent events are primarily governed by membrane-liposome interactions.

To our knowledge, no AFM imaging on liposome attachment, rupture, and spreading on a hydrophobic support has been published previously. There have, however, been many papers on the process, studied by other techniques. Kalb et al. (1992) employed total internal reflection fluorescence microscopy and found essentially the same kinetics for POPC vesicles on plain quartz slides and on a lipid-monolayer-covered slide. Plant has in several publications, recently reviewed (Plant 1999), worked with hybrid bilayers, in which the inner layer is an alkanethiol covalently bound to gold. Lipid deposition from liposomes was followed by, e.g., surface plasmon resonance. These and other authors including ourselves (Puu and Gustafson 1997) suggest a process that seems to be oversimplified, in view of the images presented here. We cannot exclude that the process could be more complex on a lipid monolayer as compared with a covalently bound hydrophobic tail, as the lipid monolayer might reorganize during the process (Solletti et al.,1996). Often, deposited monolayers are imperfect, which could be the contributing factor to the irregular edges of the membranes. The surfaces of the bilayers are not as smooth as those produced on the hydrophilic surface and may also be due to underlying imperfections in the DPPA layer filled by bilayer material. Alternatively, the DPPA hydrophilic headgroups may be randomly oriented, thus providing some stability to a bilayer to be deposited and maintained. It is in no doubt that this process must be investigated to attain a more complete understanding of the mechanisms involved in bilayer formation on hydrophobic surfaces.

The AFM is a new tool for imaging surface events under physiological conditions and in real time. Although it is the

only method of visualizing small structures such as liposomes, there are potential hazards in imaging soft biological materials. Previous studies showing lipid membranes by AFM have been collected in contact mode under a constant force (Pignataro et al., 2000; Reviakine and Brisson, 2000). In contact mode, the tip is continuously in contact with the surface it is imaging; thus, in addition to introducing a vertical force on the sample it also introduces a substantial lateral force. Müller et al. (1997) reported the tip in contact mode could induce formation of bilayer structures from liposomes when the forces were greater than 100 pN. Pignataro et al. (2000) calculated that if the tip has a vertical force of 100 pN, the resultant lateral force is over 1 nN, sufficient to drag and disrupt liposomes on the surface. Tapping Mode functions by vibrating the tip over the surface at a specific frequency, thus lightly tapping the surface. In principle, it would have different tip-sample interactions than those observed in contact mode. While the vertical force may be equal to or greater than that found in contact mode, it likely has a substantially reduced lateral force. The frequency at which the tip is tuned may assist liposome adhesion and rupture, either by introducing energy or mixing into the sample. Although we did occasionally see movement of unadsorbed liposomes along the surface, we would expect to see the whole field of view converted to membranes rapidly if the forces were substantial. As we did not see this, we concluded that the tip forces were not extensively high. In some cases we suspected that the tip might have helped initiate the process; however, once it began it continued indifferent to the tip and scan direction.

Theoretical calculations suggest that rupture occurs when the contact angle of the liposome edges exceeds a critical value. This suggests that the region most prone to indentation by tip forces would be the center of the liposome (Pignataro et al., 2000). Our results show that liposomes are slightly compressed during imaging; however, the flattening and spreading occurs from the outer edges to the center of the liposome suggesting that these forces were not substantial.

CONCLUSIONS

The need for a deeper understanding of the processes involved in adhesion, rupture, and spreading is obvious for experimentalists in the field. A common experience is that small variations in the experimental set-up often give large differences in the qualities of the final, supported membranes. If the supported membrane is intended for applications, for example, in basic research in membrane-mediated processes or as biosensors, it must be possible to govern the process in a rationale way. Important recent contributions to a deeper understanding include both simulations (Zhdanov et al., 2000) and experimental studies, coupled to theoretical aspects (Reviakine and Brisson, 2000; Pignataro et al., 2000). The present work, in which we have used sequential AFM imaging as a tool for following the process on both a hydrophilic and a hydrophobic surface, could be another building block in efforts toward useful theoretical and empirical models. Apart from gross structural changes, we could catch intermediate stages in the images.

Website

Full sequences from the experiments reported here and a few others will be available at www.foa.se/surfbiotech.

REFERENCES

Beckmann, M., P. Nollert, and H.-A. Kolb. 1998. Manipulation and molecular resolution of a phosphatidylcholine-supported planar bilayer by atomic force microscopy. *J. Membr. Biol.* 161:227–233.

Carlson, J. W., A. Jonas, and S. G. Sligar. 1997. Imaging and manipulation of high-density lipoproteins. *Biophys. J.* 73:1184–1189.

Contino, P. B., C. A. Hasselbacher, J. B. A. Ross, and Y. Nemerson. 1994. Use of an oriented transmembrane protein to probe the assembly of a supported phospholipid bilayer. *Biophys. J.* 67:1113–1116.

Csúcs, G., and J. Ramsden. 1998. Interaction of phospholipid vesicles with smooth metal-oxide surfaces. *Biochim. Biophys. Acta.* 1369:61–70.

Grandbois, M., H. Clausen-Schaumann, and H. Gaub. 1998. Atomic force microscope imaging of phospholipid bilayer degradation by phospholipase A_2. *Biophys. J.* 74:2398–2404.

Hui, S. W., R. Viswawanathan, J. A. Zasadzinski, and J. N. Israelachvili. 1995. The structure and stability of phospholipid bilayers by atomic force microscopy. *Biophys. J.* 68:171–178.

Kalb, E., S. Frey, and L. K. Tamm. 1992. Formation of supported planar bilayers by fusion of vesicles to supported phospholipid monolayers. *Biochim. Biophys. Acta.* 1103:307–312.

Keller, C. A., and B. Kasemo. 1998. Surface specific kinetics of lipid vesicle adsorption measured with a quartz crystal microbalance. *Biophys. J.* 75:1397–1402.

McConnell, H. M., T. H. Watts, R. M. Weis, and A. A. Brian. 1986. Supported planar membranes in studies of cell-cell recognition in the immune system. *Biochim. Biophys. Acta.* 864:95–106.

Mimms, L. T., G. Zampighi, Y. Nozaki, C. Tanford, and J. A. Reynolds. 1981. Phospholipid vesicle formation and transmembrane protein incorporation using octylglycoside. *Biochemistry.* 20:833–840.

Müller, D. J., M. Amrein, and A. Engel. 1997. Adsorption of biological molecules to a solid support for scanning probe microscopy. *J. Struct. Biol.* 119:172–188.

Müller, D. J., and A. Engel. 1997. The height of biomolecules measured with the atomic force microscope depends on electrostatic interactions. *Biophys. J.* 73:1633–1644.

Nikolelis, D. P., T. Hianik, and U. J. Krull. 1999. Biosensors based on thin lipid films and liposomes. *Electroanalysis.* 11:7–15.

Nollert, P., H. Kiefer, and F. Jähnig. 1995. Lipid vesicle adsorption versus formation of planar bilayers solid surfaces. *Biophys. J.* 69:1447–1455.

Pignataro, B., C. Steinem, H.-J. Galla, H. Fuchs, and A. Janshoff. 2000. Specific adhesion of vesicles monitored by scanning force microscopy and quartz crystal microbalance. *Biophys. J.* 78:487–498.

Plant, A. L. 1999. Supported hybrid bilayer membranes as rugged cell membrane mimics. *Langmuir.* 15:5128–5135.

Puu, G., E. Artursson, I. Gustafson, M. Lundström, and J. Jass. 2000. Distribution and stability of membrane proteins in lipid membranes on solid supports. *Biosensors Bioelectronics.* 15:31–41.

Puu, G., and I. Gustafson. 1997. Planar lipid bilayers on solid supports from liposomes -factors of importance for kinetics and stability. *Biochim. Biophys. Acta.* 1327:149–161.

Puu, G., I. Gustafson, E. Artursson and P.-Å. Ohlsson. 1995. Retained activities of some membrane proteins in stable lipid bilayers on a solid support. *Biosensors Bioelectronics.* 10:463–476.

Rädler, J., H. Strey, and E. Sackmann. 1995. Phenomenology and kinetics of lipid bilayer spreading on hydrophilic surfaces. *Langmuir*. 11: 4539–4548.

Reviakine, I., and A. Brisson. 2000. Formation of supported phospholipid bilayers from unilamellar vesicles investigated by atomic force microscopy. *Langmuir*. 16:1806–1815.

Roberts, G. (editor). 1990. Langmuir-Blodgett films. Plenum Press, New York.

Salafsky, J., J. T. Groves, and S. G. Boxer. 1996. Architecture and function of membrane proteins in planar supported bilayers: a study with photosynthetic reaction centers. *Biochemistry*. 35:14773–14781.

Santos, N. C., E. Ter-Ovanesyan, J. A. Zasadzinski, and M. A. R. B. Castanho. 1998. Reconstitution of phospholipid bilayer by an atomic force microscope tip. *Biophys. J.* 75:2119–2120.

Sellström, Å., I. Gustafson, P.-Å. Ohlsson, G. Olofsson, and G. Puu. 1992. On the deposition of phospholipids onto planar supports with the Langmuir-Blodgett technique using factorial experimental design. I. Screening of various factors and supports. *Coll. Surf.* 64:275–287.

Shao, Z., and J. Yang. 1995. Progress in high resolution atomic force microscopy in biology. *Quart. Rev. Biophys.* 28:195–251.

Singh, S., and D. J. Keller. 1991. Atomic force microscopy of supported planar membrane bilayers. *Biophys. J.* 60:1401–1410.

Solletti, J. M., M. Botreau, F. Sommer, W. L. Brunat, S. Kasas, T. M. Duc, and M. R. Celio. 1996. Elaboration and characterization of phospholipid Langmuir-Blodgett films. *Langmuir*. 12:5379–5386.

Zhdanov, V. P., C. A. Keller, K. Glasmästar, and B. Kasemo. 2000. Simulation of adsorption kinetics of lipid vesicles. *J. Chem. Phys.* 112:900–909.